Pertanika J. Sci. & Technol. 33 (1): 405 - 421 (2025)

PERTANIKA JOURNALS

SCIENCE & TECHNOLOGY

Journal homepage: http://www.pertanika.upm.edu.my/

Factors Controlling Durability of Geopolymer Concretes in Chloride Determined via Growing Self-Organizing Maps

Fong Wen Lee[1], Chang Wui Lee[2], Teo Siaw Hui[1], Tay Kai Meng[1], Annisa Jamali[1], Mohamad Nazim Jambli[3] and Idawati Ismail[1]*

[1]Faculty of Engineering, Universiti Malaysia Sarawak, 94300 Kota Samarahan, Sarawak, Malaysia
[2]School of Computing and Creative Media, University of Technology Sarawak, 1, Jalan University, 96000 Sibu, Sarawak, Malaysia
[3]Faculty of Computer Science and Information Technology, Universiti Malaysia Sarawak, 94300 Kota Samarahan, Sarawak, Malaysia

ABSTRACT

Geopolymer concrete offers a promising alternative to traditional Portland cement concrete, exhibiting comparable mechanical and durability performance while reducing environmental impacts. However, its mechanical and durability properties depend on many factors, such as the water/binder ratios, concentration of activator and curing temperatures. This study proposes using an unsupervised Artificial Neural Network (ANN) Self-Organizing Map (SOM) to predict the factors that control the durability of geopolymer concrete in a chloride environment based on experimental datasets. This research aims to identify the impact of various water-to-binder ratios and molarity of activators on the durability of geopolymer concretes by applying the Growing Self-Organizing Maps (GSOM) model to predict the durability of the design mix. A series of geopolymer concrete mixes with varying water-to-binder (w/b) ratios and activator molarity were prepared to achieve these goals. These cylindrical samples of 100 mm height × 50 mm diameter size were cured for 24 hours at 80°C and subject to chloride migration test at 28-day curing age. The data collected was analyzed and modeled using statistical methods and machine learning techniques, i.e., SOM modeling. This modeling approach effectively revealed patterns and relationships within the dataset, providing crucial insights into the chloride migration behavior. Based on the GSOM modeling, this study highlights efficient data analysis, pattern recognition, and optimization of outcomes, such as geopolymer concrete durability prediction in a chloride environment based on the selected parameters.

Keywords: Artificial Neural Network (ANN); durability; geopolymer concrete; Self-organizing map (SOM)

ARTICLE INFO

Article history:
Received: 8 March 2024
Accepted: 18 September 2024
Published: 27 January 2025

DOI: https://doi.org/10.47836/pjst.33.1.18

E-mail addresses:
21020482@siswa.unimas.my (Fong Wen Lee)
wui.lee@uts.edu.my (Chang Wui Lee)
21020039@siswa.unimas.my (Teo Siaw Hui)
kmtay@unimas.my (Tay Kai Meng)
jannisa@unimas.my (Annisa Jamali)
jmnazim@unimas.my (Mohamad Nazim Jambli)
iidawati@unimas.my (Idawati Ismail)
*Corresponding author

ISSN: 0128-7680
e-ISSN: 2231-8526

INTRODUCTION

Geopolymer concrete represents an innovative and sustainable paradigm in construction materials. It departs from the dependency on conventional Portland cement-based concrete by utilizing industrial byproducts, natural sources, or waste materials with high silica and alumina content, such as fly ash, slag, and metakaolin (Cong & Cheng, 2021). The precursors go through a geopolymerization process, where these source materials react with an alkaline activator solution, typically composed of sodium hydroxide (NaOH) and sodium silicate (Na_2SiO_3). During geopolymerization, these constituents undergo a chemical transformation, forming a robust three-dimensional network of interconnected polymeric chains, which serve as the binding matrix for the concrete (Gunasekara et al., 2019). This unique chemistry not only reduces the environmental footprint by diminishing carbon dioxide emissions related to traditional Portland cement production but also offers geopolymer concrete with remarkable attributes, including exceptional fire resistance (Cong & Cheng, 2021), rapid early strength development (Amran et al., 2021), and formidable resistance to chemical aggression (Wong, 2022), making it an eco-friendly and high-performance choice for various construction applications.

Chloride-induced corrosion of steel reinforcement in concrete is primarily attributed to the penetration of chloride ions into the concrete matrix. This penetration is influenced by several factors, including the chloride ion concentration at the surface of steel, with critical levels around 0.4% by weight of cement being a potential threshold for corrosion initiation (Zofia & Adam, 2013). The porosity of concrete plays a pivotal role in facilitating chloride ingress. Chloride ions permeate concrete through three key mechanisms: capillary absorption, hydrostatic pressure, and diffusion. The predominant mechanism is diffusion, driven by concentration gradients and dependent on factors such as ion concentration differences and continuous pore fluid Sirivivatnanon and Khatri (2011), and Shobeiri et al. (2021). It occurs predominantly in submerged conditions, where the concentration disparity between contaminated and uncontaminated surfaces and the diffusion coefficient determine the ingress rate. Concrete, characterized by solids and voids filled with fluid and air, can also experience chloride penetration due to hydraulic pressure caused by the presence of chloride ions at the concrete surface (Halim et al., 2017). Capillary absorption relies on moisture gradients to facilitate chloride ion movement into concrete pores (Titi & Tabatabai, 2018).

Several critical factors influence the durability of geopolymer concrete, and one of the most significant concerns is the risk of chloride-induced corrosion. This corrosion process can be complex and is influenced by several key factors (Chen et al., 2021; Chindaprasirt & Chalee, 2014). The initial chloride concentration in the environment, the exposure duration, the geopolymer concrete's specific mix design, and the prevailing environmental conditions all play vital roles (Tennakoon et al., 2017; Titi & Tabatabai, 2018).

The main aim of this study is to adopt machine learning methods to predetermine the chloride permeability durability of geopolymer concrete. Artificial intelligence (AI) is revolutionizing engineering by streamlining tasks and optimizing the design and maintenance of engineering systems. AI algorithms can efficiently analyze large datasets to recognize patterns and make predictions, offering a wide range of applications, including complex system design, predictive maintenance, and more (Huang et al., 2015). As AI technology continues to advance, it is expected to profoundly impact the field of engineering. In geopolymer concrete durability prediction in chloride-rich environments, machine learning techniques, including artificial neural networks (ANNs), support vector machines (SVMs), random forests, and decision trees, are employed to develop predictive models. These models rely on comprehensive datasets, including concrete composition, preparation techniques, testing conditions, and chloride penetration test results. The successful implementation of machine learning models has the potential to significantly enhance the safety and longevity of concrete structures by providing engineers and designers with precise insights into material behavior under varying conditions (Pavithra et al., 2016). While machine learning models can significantly contribute to our understanding, it's important to acknowledge the complexity of real-world scenarios and the need for continued research and refinement in this field.

In the field of machine learning, two fundamental approaches are supervised and unsupervised learning (Rahmatbakhsh et al., 2021). Supervised learning utilizes labeled data to learn a set of training data samples and classify them based on their labels, which is useful for precise predictions. On the other hand, unsupervised learning (often known as clustering) uncovers the hidden patterns from the set of training data samples and partitions similar patterns into a cluster of similar patterns (Padmapoorani et al., 2023). The self-organizing feature of an AI algorithm has exhibited a remarkable ability to retain the information acquired from the learning of the data samples that are used to adjust responses of presented data samples. While the labeled data samples are hardly (expensive) to be acquired in geopolymer concrete studies, clustering serves as a better alternative in this study.

The Self-Organizing Map (SOM) is adopted for its unique feature of clustering high-dimensional data onto a low-dimensional (2D) topological map. While the topological map consists of a number of nodes (clusters) that are self-organized according to the topological relationship among the data samples, visualizing the 2D topological map provides useful insights into the data structure. It potentially reveals the hidden message for knowledge discovery, especially in the geopolymer concrete study. Kalteh et al. (2008) outlined a structured approach involving data gathering and normalization, training the SOM, and extracting information from it. These steps enable visualizing data patterns, grouping data through clustering, and identifying distinct clusters for further analysis. Extracting the

hidden message from a SOM model may include deriving a rule-based model at the clusters that precisely describes and/or predicts geopolymer concrete's diffusion coefficient across various mixing designs. Ensuring the consistency of mixed designs with experimental data and assessing the reliability of these designs in guiding specific chloride permeability levels are crucial. It is particularly significant given the potential variations and parameters that may not be explicitly accounted for in the training data (Colantonio et al., 2021).

The adoption of SOM extends to the design of geopolymer concretes, with researchers exploring its structural potential, driven by the growing interest in SOM clustering. The previous focus of the geopolymer concrete study included analyzing micro-scale materials like the composition and structure of aluminosilicate precursors, the distribution of reaction products, and the development of pore structures at the micro level. Based on these findings, current research trends are focused on investigating the performance of nano-silica or nano-alumina additives on the microstructure and properties of geopolymer concrete at a larger scale (Mayhoub et al., 2021). Additionally, there is growing interest in studying the influence of activator solution concentration at the micro level and the impact of curing temperature on microstructural development, as these factors could offer valuable insights into the material's behavior in practical construction applications. Among the researchers, the geopolymer concrete durability characteristics are of most interest, particularly in the impact of chloride attack (Pasupathy et al., 2021) on compressive strength and chloride binding capacity of fly ash geopolymers under varied curing conditions.

Limited research papers reportedly refine the geopolymer concrete parameter settings to enhance strength (Mohammed et al., 2021), durability (Huseien & Shah, 2020) and energy efficiency (Chen et al., 2021). Therefore, the development of the SOM model can reveal the underlying information, such as mixed proportions. The modeling uses geopolymer concrete data, such as compressive strength or penetration depth of ionic species. This paper explores how SOM models predict the durability of fly ash geopolymer concretes in chloride.

EXPERIMENTAL METHOD

Raw Materials

The raw precursor used in this study is Class F fly ash obtained from Sejingkat Power Station, Kuching, Sarawak, Malaysia. The chemical composition of the raw material is shown in Table 1 and was classified according to ASTM C618. Two types of alkaline were used in a combination of NaOH and sodium silicate (Na_2SiO_3) at a 1:0.5 mass ratio. Only coarse aggregates of 20 mm maximum size were used to ensure homogeneity and fine aggregates were also used through a 4.75mm sieve.

Table 1
Chemical composition of fly ash by XRF (%)

Precursor	MgO	Al2O3	SiO2	P2O5	SO3	K2O	CaO	TiO2	MnO	Fe2O3	Rb2O2	SrO	ZrO
Fly Ash	0.5	15.7	53	1.44	0.144	4.71	5.21	1.57	0.295	17.1	0.081	0.372	0.000ppm

Table 2
Mix Proportions for Chloride Permeability Test

No.	Liquid to Binder ratio	Molarity	Sodium Hydroxide to Sodium Silicate ratio	Aggregate kg,(kg/m³)	Sand kg,(kg/m³)	Fly Ashes kg,(kg/m³)	NaOH (kg)	Na_2SiO_3 (kg)	Water (ml)
1	0.3	8	1:0.5	12.965(2400)	6.485(1600)	3.23 (540)	0.311	0.155	972
2	0.4	8	1:0.5	12.965(2400)	6.485(1600)	3.23(540)	0.414	0.207	1296
3	0.5	8	1:0.5	12.965(2400)	6.485(1600)	3.23(540)	0.518	0.259	1620
4	0.3	10	1:0.5	12.965(2400)	6.485(1600)	3.23(540)	0.388	0.194	972
5	0.4	10	1:0.5	12.965(2400)	6.485(1600)	3.23(540)	0.518	0.259	1296
6	0.5	10	1:0.5	12.965(2400)	6.485(1600)	3.23(540)	0.648	0.324	1620
7	0.3	12	1:0.5	12.965(2400)	6.485(1600)	3.23(540)	0.466	0.233	972
8	0.4	12	1:0.5	12.965(2400)	6.485(1600)	3.23(540)	0.622	0.311	1296
9	0.5	12	1:0.5	12.965(2400)	6.485(1600)	3.23(540)	0.780	0.390	1620

Samples and Testing

Table 2 shows the mixed proportions to make the fly ash geopolymer concretes. The geopolymer concrete was mixed using a concrete mixer, cast into a 100 mm × 200 mm height cylinder mold and vibrated using a vibrator for about 15 s. This vibration process was to ensure that the geopolymer concrete was fully compacted. Then, the samples were cured at 80°C for 24 h in a curing oven. After demolding, the samples were sealed to prevent moisture loss until the age of testing, which is on day 28 for the chloride migration test. A total of 162 samples were prepared as training data sets.

Chloride Diffusion Experiment

The diffusion of chloride was conducted according to non-steady state migration—NT BUILD 492 (Nordic Council of Ministers, 1999). Figure 1 shows the experiment setup, which uses external electrical potential to allow chloride ions to penetrate the specimen. After 24 hours, the specimens were split and sprayed with silver nitrate solution. The white precipitates indicate the presence of silver chloride precipitates at the split surface, indicating chloride penetration.

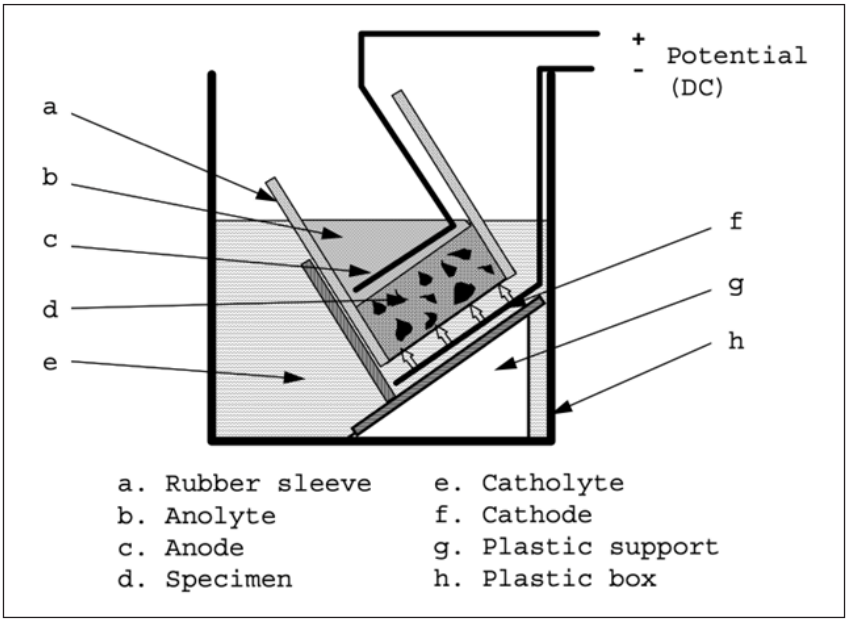

Figure 1. Nord Test Method Sample Migration Setup

Figure 2 compares chloride penetration depth and chloride diffusion coefficients in geopolymer samples as a function of water-to-binder ratios and molarity. These data sets from 162 samples were used in the SOM prediction model.

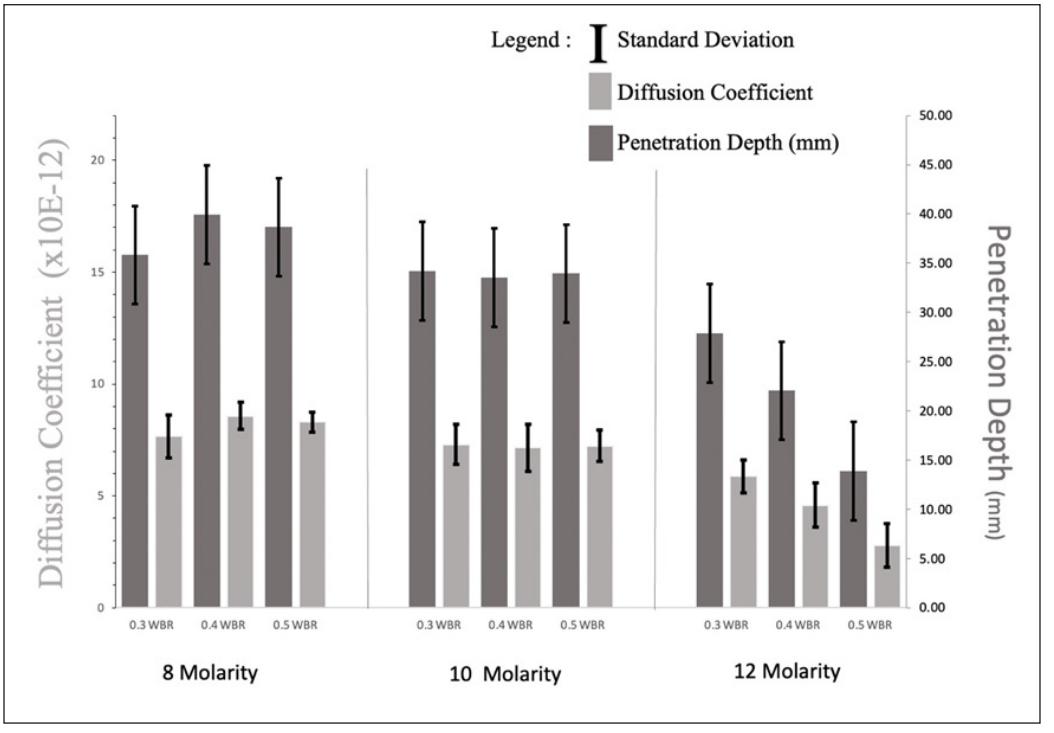

Figure 2. Chloride Penetration Depth and Coefficients as a function of w/b ratio and molarity

Self-Organizing Maps (SOM)

In this study, Self-Organizing Maps (SOM) are pivotal in determining the optimal mixing design for geopolymer concrete. The dataset used in this analysis has been meticulously assembled through rigorous experiments and testing procedures. An array of activator mixing design variations was systematically applied to geopolymer concrete samples. In total, this comprehensive approach encompassed a total of 162 individual specimens. Each of these distinct combinations underwent chloride permeability testing after a 28-day curing period. This dataset serves as the cornerstone for SOM analysis, enabling in-depth exploration of the intricate relationships between mixing design elements and chloride permeability (Stryhal & Plavcová, 2023). Data preprocessing, a vital step in any analytical process, including SOM modeling, involves meticulous data preparation, quality assurance, and necessary transformations. In this particular study, data preprocessing incorporates a normalization procedure, which scales the data to a standardized range to ensure that all variables contribute equally to shaping the SOM model (Alahakoon et al., 2000). Data preprocessing is instrumental because variables may have dissimilar scales, and normalization mitigates the risk of one variable overshadowing others due to its larger values (Mehta et al., 2017).

Growing Self-Organizing Maps (GSOM) is a variant of Self-Organizing Maps (SOM) that can dynamically adjust their size during learning. Unlike traditional SOMs, GSOMs can grow or shrink in response to the input data, allowing them to adapt and represent complex structures more effectively (Alahakoon et al., 2000). The primary advantage of GSOM is its capability to automatically expand the map size in regions of high data density, thereby enhancing its ability to capture intricate patterns.

The GSOM begins by normalizing a dataset from a collection data sample to a range of [0,1]. Then, a map size of (1×1) is initiated, where the initial prototype weight vector is randomly assigned within the normalized data space. Then, SOM's learning process is conducted by fetching one data sample at a time. Similarity measures are conducted, using Equation 1, on the data sample to determine the best-matching-unit (BMU) among the nodes in the map size. Then, update the BMU node to move the node towards the data sample using Equations 2 and 3. Repeat the SOM's learning process by fetching the next data sample until all data samples are learned. Learning of the normalized data samples is repeated at the next learning epoch(s) until the prototype weight vectors are converged (i.e., no changes after each learning). Determine a hit sample count at all nodes to identify a row (or column) of maximum hit sample counts from the map size. Duplicate the identified row (or column) nodes' prototype weight vectors with a new row (or column) of nodes that are positioned next to the identified row (or column) to increase the map size. Repeat the SOM's learning process until the maximum hit sample counts (in row and column nodes) are less than a preset threshold value.

The proposed GSOM procedure for geopolymer concrete analysis involves mainly nine steps.

In step 1, the GSOM is initialized with two nodes or clusters, where a random valued prototype weight vector, $\boldsymbol{w}_j = [w_{j,1}, \ldots, w_{j,p}], j = \{1,2\}$, is assigned as the centroid of the cluster.

In step 2, a collected data set is fed for learning on the cluster created. The data set consists of n data samples of p parameter settings of water/binder ratio, molarity, activator NaOH, activator Na_2SiO_3, water, and chloride diffusion coefficient, where each parameter value is normalized to a range of [0,1] to ease the similarity test in the next step. The normalizing method divides the real parameter value by a maximum constant.

In step 3, the learning of GSOM begins with a similarity test on a data sample, $\boldsymbol{x}_i = [x_{i,1}, \ldots, x_{i,p}]$, on the available clusters using Equation 1.

$$d(\boldsymbol{x}_i, \boldsymbol{w}_j) = \sqrt[2]{\sum_{k=1}^{p} (x_{i,k} - w_{j,k})^2} \quad [1]$$

Step 9 selects a winner, *J*, among the clusters using Equation 2.

$$J = \arg\min_j d(\boldsymbol{x}_i, \boldsymbol{w}_j) \quad [2]$$

In step 5, the winner cluster and its adjacent clusters are updated with Equations 3 and 4, where h_{jJ} is the topological-based learning rate that is obtained by calculating the distance between the adjacent *J*-th node (N_j) and winner *J*-th node (N_J) on the topological map. Let $j = J$ of Equation 3 update the winner cluster's prototype weight vector, and h_{jJ} of Equation 4 is at the maximum of the learning rate ($h_{jJ} = \alpha$). At the same time, an adjacent node's prototype weight vector ($\boldsymbol{w}_j$) is updated with a lower $h\_JJ < \alpha$ for the self-organizing feature. $\alpha, \sigma \in [0,1]$ are the learning rate and adjacent width that are monotonically reduced over the period of learning.

$$\boldsymbol{w}_j = \boldsymbol{w}_j + h_{jJ}(\boldsymbol{x}_i - \boldsymbol{w}_j) \quad [3]$$

$$h_{jJ} = \alpha \exp\left(-\left(N_j - N_J\right)^2 / 2\sigma^2\right) \quad [4]$$

In step 6, a hit sample counter of N_J is incremented to determine the size of the cluster.

In step 7, go to step 2 with the subsequent data sample $\boldsymbol{x}_{\_i}, i = i + 1$, until $i = n$.

In step 8, the hit sample counters are evaluated for the growth of nodes. A row or a column of new nodes is inserted to retain the topological feature of the previous map. The row of nodes is inserted to the west side of the row with the maximum total hit sample counts, and their prototype weight vectors are initiated from the rows. Otherwise, a column of nodes is inserted to the north side of the column with the maximum total hit sample counts, and their prototype weight vectors are initiated from the columns.

In step 9, go to step 2 fetch $\boldsymbol{x}_i, i = 1$.

These steps are recursively conducted until the hit sample count of all nodes does not exceed the maximum count. Figure 3 summarizes the overall steps.

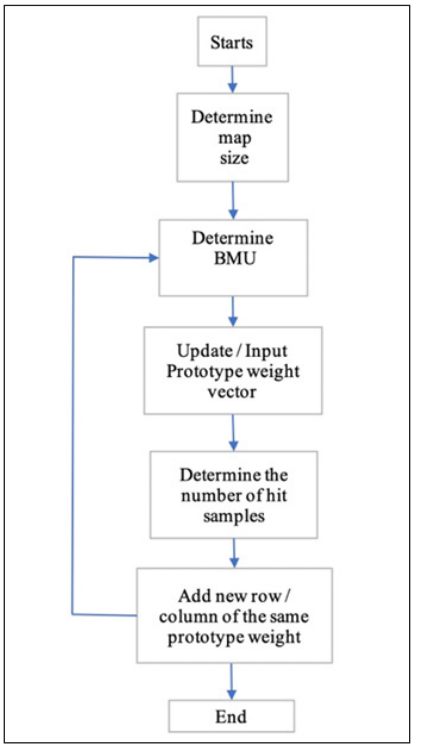

Figure 3. Flow chart of Growing SOM

RESULTS AND DISCUSSION

SOM Simulation

From MATLAB, the SOM model was trained using a 5 × 5 map size, resulting in a grid of 25 neurons arranged in a hexagonal structure, as shown in Figure 4. Each neuron represented specific combinations of activator dosages and chloride permeability. The hexagonal topology allowed information exchange between adjacent neurons, aiding self-organization and learning.

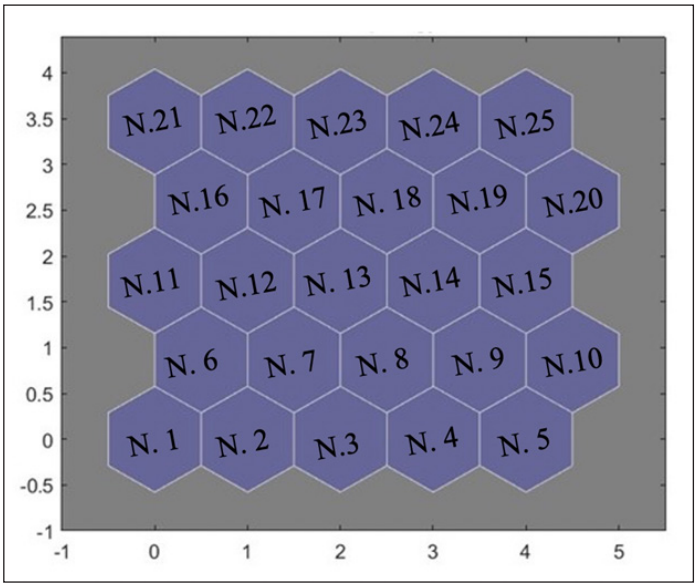

(a)

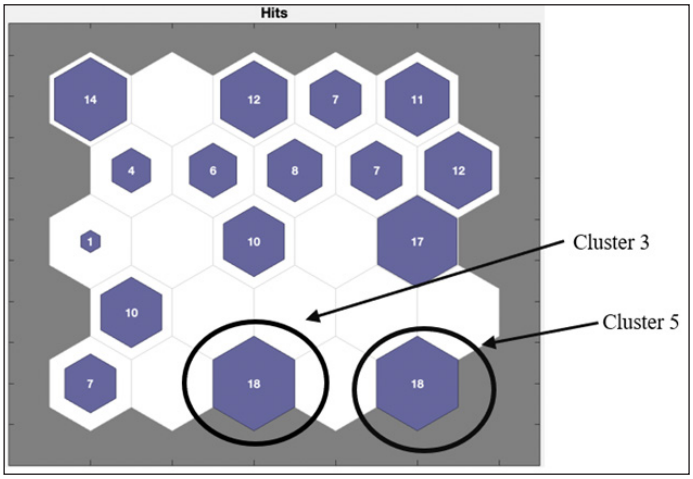

(b)

Figure 4. Self-organizing map (SOM) topology; (a) 5 × 5 map and (b) hit map

Hit maps were generated, as per Figures 4(a) and 4(b), revealing how the input data was distributed within clusters to assess the model's effectiveness. These maps also assessed the quality of clustering, with clusters 3 and 5 receiving more hits, indicating their better representation of common patterns in the data. However, some clusters lacked associated datasets, suggesting that the chosen number of clusters may not have been ideal for capturing distinct variations in the data. Overall, SOM analysis offered valuable insights into mixing design patterns, emphasizing the importance of precise mix design considerations to achieve durable and structurally sound geopolymer concrete compositions.

Meanwhile, the SOM neighbor weight distance analysis assesses the likeness or disparity between neighboring neuron weight vectors, determining the input's influence on each neuron's output (Figure 5). The weight distances were calculated using the Euclidean distance of Equation 1.

Using the SOM library in MATLAB, these neighbor weight distances are visualized using a colormap, as depicted in Figure 5. The dark shade represents the least relevance between the nodes, while the light shade represents the highest relevance of the nodes. This colormap provides a graphical illustration for identifying clusters of similar information or the relevant geopolymer concrete characteristics. For instance, *r_9* and *r_10* are the relevant nodes indicated in the colormap figure.

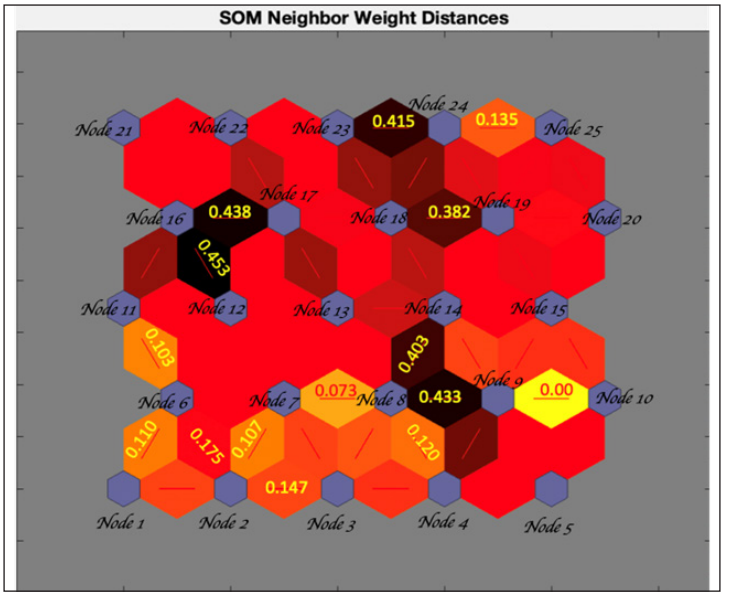

Figure 5. SOM neighbor weight distances

Deriving insights from a trained SOM requires some post-processing to create a cluster "recipe" or mix proportion chosen for its accuracy in predicting the durability of geopolymer

concrete under various chloride exposure conditions. Ensuring alignment with experimental data and providing reliable recommendations for achieving specific durability levels is crucial. The recipe's robustness is also considered, aiming to offer reliable suggestions for datasets beyond those used for training.

Prediction from SOM

Table 3 shows the prototype weight vectors of SOM, but Table 4 illustrates their implications. Each element of the prototype weight vectors is interpreted in terms of the water/binder ratio, molarity, water volume in units of ml, NaOH in units of g, and chloride diffusion coefficient in units of m^2/s parameters, respectively.

Table 3
Weight vectors of 5x5 nodes rounded to the nearest 4 decimal places from SOM in MATLAB

j	$w_{j,1}$	$w_{j,2}$	$w_{j,3}$	$w_{j,4}$	$w_{j,5}$	$w_{j,6}$
1	1	0.6667	0.6641	0.6641	1	0.8546
2	0.8947	0.6686	0.6115	0.6115	0.8947	0.8678
3	0.8000	0.6667	0.5308	0.5308	0.8000	0.8916
4	0.6909	0.6667	0.4587	0.4580	0.6909	0.8355
5	0.6000	0.6667	0.3987	0.3974	0.6000	0.8174
6	0.9744	0.7564	0.7325	0.7325	0.9744	0.8118
7	0.8000	0.8333	0.6641	0.6641	0.8000	0.8237
8	0.8000	0.7500	0.5974	0.5974	0.8000	0.8127
9	0.6000	0.6667	0.3987	0.3974	0.6000	0.4619
10	0.6000	0.6667	0.3987	0.3974	0.6000	0.6702
11	1	0.8333	0.8308	0.8308	1	0.7429
12	0.8974	0.8675	0.7754	0.7754	0.8974	0.7049
13	0.8000	0.8333	0.6641	0.6641	0.8000	0.6459
14	0.6741	0.8457	0.5666	0.5666	0.6741	0.7314
15	0.6000	0.8333	0.4974	0.4974	0.6000	0.7951
16	1	1	1	1	1	0.4399
17	0.8000	1	0.7974	0.7974	0.8000	0.6032
18	0.8000	0.8333	0.6641	0.6641	0.8000	0.5438
19	0.6000	1.0000	0.5974	0.5974	0.6000	0.6462
20	0.6000	0.8333	0.4974	0.4974	0.6000	0.6525
21	1	1	1	1	1	0.2347
22	0.9034	1.0000	0.9022	0.9022	0.9034	0.3885
23	0.8000	1	0.7974	0.7974	0.8000	0.4155
24	0.6667	1.0000	0.6641	0.6641	0.6667	0.5433
25	0.6000	1	0.5974	0.5974	0.6	0.5404

Table 4
Predicted chloride diffusion coefficients from SOM 5 × 5 nodes

Cluster	WBR	Molarity	NaOH (g)	Na_2SiO_3 (g)	Water (ml)	Chloride Diffusion Coefficient (m^2/s)
1	0.5	10	648	324	1620	$1.8170e^{-11}$
2	0.5	8.9697	581.0303	290.5152	1620	$1.7847e^{-11}$
3	0.5	8.0000	518.0000	259.0000	1620	$1.8673e^{-11}$
4	0.4548	8.0000	471.0323	235.5161	1473	$1.9165e^{-11}$
5	0.4	8.0000	414	207	1296	$1.9443e^{-11}$
6	0.5	10.0000	648	324	1620	$1.5490e^{-11}$
7	0.4658	9.1053	545.3684	272.6842	1509	$1.7656e^{-11}$
8	0.4567	8.8667	518.0000	259.0000	1479	$1.8233e^{-11}$
9	0.3452	8.0000	357.5161	178.4839	1118	$1.8592e^{-11}$
10	0.3452	8.0000	357.5161	178.4839	1118	$1.8592e^{-11}$
11	0.5	10	648	324	1620	$1.3425e^{-11}$
12	0.4400	10.5333	600.5333	300.2667	1425	$1.5398e^{-11}$
13	0.4000	10.000	518.0000	259.0000	1296	$1.8148e^{-11}$
14	0.3400	9.1000	405.3500	202.4500	1101	$1.6593e^{-11}$
15	0.3000	8	311.0000	155.0000	972	$1.7699e^{-11}$
16	0.5000	12	780	390	1620	$9.6929e^{-12}$
17	0.4000	12.0000	622	311	1296	$1.3216e^{-11}$
18	0.4000	10	518	259	1296	$1.3857e^{-11}$
19	0.3000	9.7143	377.0000	188.4286	972	$1.3776e^{-11}$
20	0.3000	10.000	388	194	972	$1.7781e^{-11}$
21	**0.5000**	**12**	**780**	**390**	**1620**	**$5.3012e^{-12}$**
22	0.4515	12.0000	703.3939	351.6970	1462	$8.4333e^{-12}$
23	0.4000	12	622	311	1296	$9.0224e^{-12}$
24	0.3000	12	466	233	972	$1.1914e^{-11}$
25	0.3000	12	466	233	972	$1.4555e^{-11}$

The SOM reveals suggestions on the lowest possible chloride diffusion coefficient in the formulation of geopolymer concrete. This geopolymer mix has a water/binder ratio of 0.5 coupled with a molarity of 12, as per the above SOM suggested. The optimal combination is cluster 21 (highlighted in bold), as depicted in Table 4, with the lowest chloride penetration depth and diffusion coefficient.

Verification and Validation

The cluster formula obtained from the clustering analysis underwent a 5-fold cross-validation process to confirm its reliability and evaluate the accuracy of the suggested mixing design and activator dosage in predicting chloride permeability. Two key validation metrics were employed: the mean absolute error (MAE) and the coefficient of determination

(R^2). The MAE and R^2 results were recorded as $1.515e^{-12}$ and 0.77, respectively, demonstrating that the cluster formula effectively forecasts chloride permeability based on the recommended mixing design. These validation outcomes are still confident in the cluster formula's capacity to guide selecting the ideal mixing design and activator dosages, ensuring the desired chloride resistance in geopolymer fly ash concrete. Figure 6 illustrates these validation results.

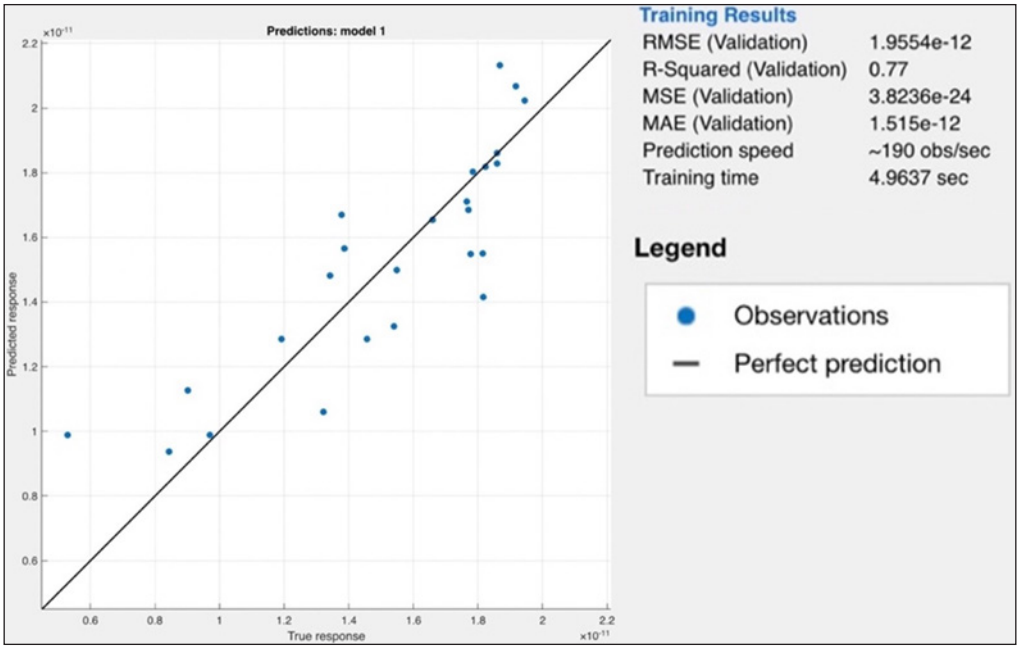

Figure 6. Performance of the clustering formula generated from the clustering analysis

CONCLUSION

The application of SOM analysis offers a systematic and efficient method to examine a vast dataset comprising formulas and their associated diffusion coefficients. By utilizing AI technology, the analysis can unveil hidden patterns, relationships, and clusters within the data that may not be easily discernible using conventional approaches. This ability to uncover meaningful insights from complex datasets enhances the overall effectiveness and efficiency of the decision-making process.

This study demonstrates the significant advantages of utilizing AI technologies, specifically Self-Organizing Maps (SOM), for efficient data analysis and pattern recognition in material science.

1. Efficient Data Analysis: AI technologies like SOM enable swift and effective processing of large, complex, and multidimensional datasets. It allows for the identification of patterns and relationships that are difficult to detect manually.

2. Pattern Recognition: SOM analysis revealed that a 0.5 water/binder ratio combined with 12M NaOH consistently resulted in the lowest diffusion coefficients. This pattern recognition capability aids decision-making by highlighting the most effective factors or combinations.
3. Optimization and Resource Efficiency: AI technology helps optimize formulas for desired outcomes, such as reducing diffusion coefficients. It leads to efficient use of materials, reduced costs, and minimized waste, thereby improving overall efficiency and sustainability.

By utilizing SOM in AI training, geopolymer concrete researchers and engineers can gain valuable insights into factors influencing durability, such as chloride diffusion, carbonation, and strength development. The SOM algorithm's ability to visualize and cluster data assists in comprehending the complex interactions within the material, ultimately enhancing the accuracy and effectiveness of AI models in predicting geopolymer concrete durability.

ACKNOWLEDGEMENT

The authors acknowledged the financial support from the Ministry of Higher Education Malaysia through the Fundamental Research Grant Scheme (FRGS) FRGS/1/2020/TK01/UNIMAS/03/1.

REFERENCES

Alahakoon, D., Halgamuge, S. K., & Srinivasan, B. (2000). Dynamic self-organizing maps with controlled growth for knowledge discovery. *IEEE Transactions on Neural Networks*, *11*(3), 601–614. https://doi.org/10.1109/72.846732

Amran, M., Al-Fakih, A., Chu, S. H., Fediuk, R., Haruna, S., Azevedo, A., & Vatin, N. (2021). Long-term durability properties of geopolymer concrete: An in-depth review. *Case Studies in Construction Materials*, *15,* Article e00661. https://doi.org/10.1016/j.cscm.2021.e00661

Chen, K., Wu, D., Xia, L., Cai, Q., & Zhang, Z. (2021). Geopolymer concrete durability subjected to aggressive environments - A review of influence factors and comparison with ordinary Portland cement. *Construction and Building Materials*, *279,* Article 122496. https://doi.org/10.1016/j.conbuildmat.2021.122496

Chindaprasirt, P., & Chalee, W. (2014). Effect of sodium hydroxide concentration on chloride penetration and steel corrosion of fly ash-based geopolymer concrete under marine site. *Construction and Building Materials, 63*, 303–310. https://doi.org/10.1016/j.conbuildmat.2014.04.010

Colantonio, L., Equeter, L., Dehombreux, P., & Ducobu, F. (2021). A systematic literature review of cutting tool wear monitoring in turning by using artificial intelligence techniques. *Machines*, *9*(12), Article 351. https://doi.org/10.3390/machines9120351

Cong, P., & Cheng, Y. (2021). Advances in geopolymer materials: A comprehensive review. *Journal of Traffic and Transportation Engineering, 8*(3), 283–314. https://doi.org/10.1016/j.jtte.2021.03.004

Gunasekara, C., Law, D., Bhuiyan, S., Setunge, S., & Ward, L. (2019). Chloride induced corrosion in different fly ash based geopolymer concretes. *Construction and Building Materials*, *200*, 502–513. https://doi.org/10.1016/j.conbuildmat.2018.12.168

Halim, L. N., Ekaputri, J. J., & Triwulan. (2017). The influence of salt water on chloride penetration in geopolymer concrete. *MATEC Web of Conferences*, *97*, Article 01002. https://doi.org/10.1051/matecconf/20179701002

Huang, Q., Wang, C., Yang, C., Zhou, L., & Yin, J. (2015). Accelerated sulfate attack on mortars using electrical pulse. *Construction and Building Materials, 95*, 875–881. https://doi.org/10.1016/j.conbuildmat.2015.07.034

Huseien, G. F., & Shah, K. W. (2020). Durability and life cycle evaluation of self-compacting concrete containing fly ash as GBFS replacement with alkali activation. *Construction and Building Materials*, *235*, Article 117458. https://doi.org/10.1016/j.conbuildmat.2019.117458

Kalteh, A. M., Hjorth, P., & Berndtsson, R. (2008). Review of the self-organizing map (SOM) approach in water resources: Analysis, modelling and application. *Environmental Modelling and Software, 23*(7), 835–845. https://doi.org/10.1016/j.envsoft.2007.10.001

Mayhoub, O. A., Mohsen, A., Alharbi, Y. R., Abadel, A. A., Habib, A. O., & Kohail, M. (2021). Effect of curing regimes on chloride binding capacity of geopolymer. *Ain Shams Engineering Journal*, *12*(4), 3659–3668. https://doi.org/10.1016/J.ASEJ.2021.04.032

Mehta, A., Siddique, R., Singh, B. P., Aggoun, S., Łagód, G., & Barnat-Hunek, D. (2017). Influence of various parameters on strength and absorption properties of fly ash based geopolymer concrete designed by Taguchi method. *Construction and Building Materials*, *150*, 817–824. https://doi.org/10.1016/j.conbuildmat.2017.06.066

Mohammed, A. A., Ahmed, H. U., & Mosavi, A. (2021). Survey of mechanical properties of geopolymer concrete: A comprehensive review and data analysis. *Materials*, *14*(16), Article 4690. https://doi.org/10.3390/ma14164690

Nordic Council of Ministers (1999). C*oncrete, mortar and cement-based repair materials: Chloride migration coefficient from non-steady-state migration experiments* (Report No. NT BUILD 492). Nordic Council of Ministers

Padmapoorani, P., Senthilkumar, S., & Mohanraj, R. (2023). Machine learning techniques for structural health monitoring of concrete structures: A systematic review. *Iranian Journal of Science and Technology - Transactions of Civil Engineering*, *47*(4), 1919–1931. https://doi.org/10.1007/s40996-023-01054-5

Pasupathy, K., Sanjayan, J., Rajeev, P., & Law, D. W. (2021). The effect of chloride ingress in reinforced geopolymer concrete exposed in the marine environment. *Journal of Building Engineering*, *39*, Article 102281. https://doi.org/10.1016/j.jobe.2021.102281

Pavithra, P., Srinivasula Reddy, M., Dinakar, P., Hanumantha Rao, B., Satpathy, B. K., & Mohanty, A. N. (2016). A mix design procedure for geopolymer concrete with fly ash. *Journal of Cleaner Production, 133*, 117–125. https://doi.org/10.1016/j.jclepro.2016.05.041

Rahmatbakhsh, M., Gagarinova, A., & Babu, M. (2021). Bioinformatic analysis of temporal and spatial proteome alternations during infections. *Frontiers in Genetics*, *12*, Article 667936. https://doi.org/10.3389/fgene.2021.667936

Shobeiri, V., Bennett, B., Xie, T., & Visintin, P. (2021). A comprehensive assessment of the global warming potential of geopolymer concrete. *Journal of Cleaner Production*, *297*, Article 126669. https://doi.org/10.1016/j.jclepro.2021.126669

Sirivivatnanon, V., & Khatri, R. (2011, October). Testing and specifying chloride resistance of concrete. In *8th Austroads Bridge Conference* (pp. 472-487). Sydney, Australia.

Stryhal, J., & Plavcová, E. (2023). On using self-organizing maps and discretized Sammon maps to study links between atmospheric circulation and weather extremes. *International Journal of Climatology*, *43*(6), 2678–2698. https://doi.org/10.1002/joc.7996

Tennakoon, C., Shayan, A., Sanjayan, J. G., & Xu, A. (2017). Chloride ingress and steel corrosion in geopolymer concrete based on long term tests. *Materials and Design, 116*, 287–299. https://doi.org/10.1016/j.matdes.2016.12.030

Titi, H. H., & Tabatabai, H. (2018). Effect of coarse aggregate type on chloride ion penetration in concrete. *Construction and Building Materials*, *162*, 871–880. https://doi.org/10.1016/j.conbuildmat.2018.01.090

Wong, L. S. (2022). Durability performance of geopolymer concrete: A review. *Polymers, 14*(5), Article 868. https://doi.org/10.3390/polym14050868

Zofia, S., & Adam, Z. (2013). Theoretical model and experimental tests on chloride diffusion and migration processes in concrete. *Procedia Engineering*, *57*, 1121–1130. https://doi.org/10.1016/j.proeng.2013.04.141